# Theoretical Study of the Change in the Magnetism and Conductivity of Diethylspirobiphenalenyl

Mao Takenaka,* Takeshi Taniguchi, Takashi Kawakami, Yasutaka Kitagawa,
Mitsutaka Okumura, and Kizashi Yamaguchi
*Department of Chemistry, Graduate School of Science, Osaka University,*
*1-1 Machikaneyama-cho, Toyonaka, Osaka 560-0043*

(Received May 23, 2007; CL-070555; E-mail: takenaka@chem.sci.osaka-u.ac.jp)

The $J$ values of the Heisenberg model and $t$ and $U_{\mathrm{eff}}$ values in the Hubbard model have been evaluated by the Kohn–Sham density functional theory (KS-DFT) for dimeric pairs of diethyl-spirobiphenalenyl. The Quantum Monte Carlo (QMC) simulation has been carried out with the calculated $J$ values to evaluate the magnetic susceptibility for this molecular crystal, reproducing the experimental tendency. The band gaps estimated by using $t$ and $U_{\mathrm{eff}}$ values are also consistent with the experiment on conductivity.

Spirobiphenalenyls are organic neutral radicals containing two phenalenyls binding with the spiro junction, the center of which is a boron atom.[1,2] The $\pi$ electrons on the two phenalenyls can conjugate through the spiro junction. According to Haddon's group, 1,1′-diethyl-2,2′-spirobi(2,3-dihydro-1*H*-3-oxa-1-aza-2-borapyrene) radical crystal (**1**) exhibited the increase of molar paramegnetic susceptibility by about three times and the decrease of conductivity by about double digits around the critical temperature ($T_{\mathrm{C}} \approx 120\,\mathrm{K}$).[3]

Our group has already reported the mechanism of the change in the magnetism and conductivity for **1**.[4] The intermolecular $J$ values for the $\pi$ dimers at several temperatures were calculated by using KS-DFT. It was concluded that the coexistence of both ferro- and antiferromagnetic interactions leads to the paramagnetic behavior above the crossover temperature (around $T_{\mathrm{C}}$).

In this work, the magnetic susceptibility ($\chi_{\mathrm{p}}$) of **1** is simulated by the QMC with using the calculated $J$ values and compared with the experimental measurement. The band gaps related to conductivity were also estimated by the calculated transfer integral ($t$) and effective on-site Coulomb integral ($U_{\mathrm{eff}}$) in the Hubbard model.

The dimeric pairs of **1** are separated into two groups: $\pi$ dimers and not-$\pi$ dimers. The structures of $\pi$ dimers of **1** were obtained from the X-ray crystallographic data measured at 100 and 173 K in Cambridge Structural Database, and they were denoted by **100$\pi$** and **173$\pi$**, respectively (see Figure 1). The molecule in the $\pi$ dimer is stacked with the other in the superposition, where the major $\pi$ orbitals on the phenalenyl moieties overlap each other. The intermolecular distance varies from 3.18 to 3.31 Å with the increase of temperature.

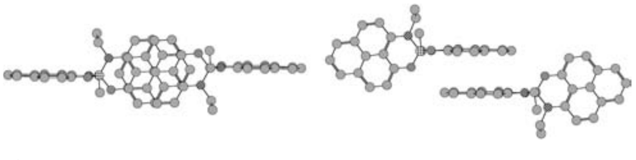

**Figure 1.** Structures of dimeric pairs of **1**: **100$\pi$** (left) and **173$\pi$** (right).

The structures of the other dimeric pairs (not-$\pi$ dimers) of **1** at 100 and 173 K were labeled by **100-1**, **100-2**, **173-1**, and **173-2** (see Figure 2). These dimeric pairs consist of a molecule nearest to a $\pi$ dimer and the half of the $\pi$ dimer.

The KS-DFT was employed to elucidate electronic structures of **1**. It can be understood that this system exhibits the spin polarization because these dimeric pairs have the closest contacts longer than van der Waals radii of carbon atom at each temperature. Here, Becke's three parameter exchange and Lee, Yang, and Parr's correlation functionals (UB3LYP) were chosen for our calculations in Gaussian98 program packages.[5]

For unrestricted calculations, broken symmetry approach with our spin projected scheme,[6] which eliminates spin contamination, can calculate the $J$ values with the following equation:

$$J = -\frac{{}^{\mathrm{HS}}E(X) - {}^{\mathrm{LS}}E(X)}{{}^{\mathrm{HS}}\langle \mathbf{S}^2 \rangle - {}^{\mathrm{LS}}\langle \mathbf{S}^2 \rangle}, \tag{1}$$

where $E(X)$ and $\langle \mathbf{S}^2 \rangle$ denote total energy and total spin angular momentum, respectively. The positive (negative) $J$ means ferromagnetic (antiferromagnetic) interaction.

The extended Hubbard model describes electron transfer by the parameters $t$ and $U_{\mathrm{eff}}$. For the two spin site, the relationship between the $J$, $t$ $(= \kappa s)$ and $U_{\mathrm{eff}}$ are derived as

$$J = \frac{U_{\mathrm{eff}}}{4} - \sqrt{\left(\frac{U_{\mathrm{eff}}}{4}\right)^2 + (\kappa s)^2}, \tag{2}$$

where $s$ means the overlap between orbitals at each site.[7]

The $\chi_{\mathrm{p}}$ was simulated on the basis of these calculated $J$ values by the loop algorithm on the ALPS project.[8]

Table 1 lists $J$ values for the dimeric pairs of **1** at 100 and 173 K. The $J$ of the $\pi$ dimers at 100 K is greatly negative, whereas its amplitude decreases at 173 K. On the other hand, magnetic interactions of **100-1** and **100-2** have been evaluated to be almost zero, suggesting that no magnetic interactions exist between spins of the dimeric pairs. **173-1**, however, has exhibited rather strong ferromagnetic interaction ($J = 187.2\,\mathrm{K}$), while **173-2** has had a very weak ferromagnetic interaction ($J = 8.3\,\mathrm{K}$). This difference between $J$ values is caused by the exchange potential effect due to the spatial arrangements of the molecules.[9] The

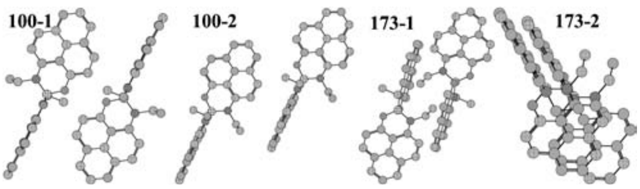

**Figure 2.** Structures of dimeric pairs of **1**: not-$\pi$ dimers.

**Table 1.** $J$ and $t$ values of the dimeric pairs for 100 and 173 K

| Models | $J$/K | $t$/eV | Models | $J$/K | $t$/eV |
|---|---|---|---|---|---|
| **100$\pi$** | −638.5 | 0.14 | **173$\pi$** | −192.1 | 0.074 |
| **100-1** | 0.3 | — | **173-1** | 187.2 | — |
| **100-2** | 0.3 | — | **173-2** | 8.3 | — |

phenalenyl moieties of each molecule are separated from each other for all not-$\pi$ dimers, except **173-1** where those moieties orientate perpendicularly (side-by-side stacking),[10] leading to the no orbital overlap. This result has indicated that the magnetic interactions cancel out as a whole and that **1** becomes paramagnetic at 173 K.

By using the calculated $J$ values, the $\chi_p$'s were evaluated for **1** by QMC as a function of temperature, on the basis of the following models: dimer lattice with $J = -639$ K for a model of the structure at 100 K and ladder lattice with $J_1 = 187$ K along the leg and $J_2 = -192$ K at the rung for a model of the structure at 173 K (see Figure 3A). Both models include $S = 1/2$ spins with periodic boundary condition.

Figure 3B illustrates variations of the calculated $\chi_p$ with the temperature ($T$). The $\chi_p$ value is almost zero for the dimer model responsible for Peierls dimerization at low temperature. It remains to be about $0.06 \times 10^{-3}$ emu mol$^{-1}$ at 120 K, though its experimental value was large (about $0.2 \times 10^{-3}$ emu mol$^{-1}$).

The peak of the $\chi_p$ vs. $T$ plots for the ladder model is found around 130 K, and its magnetitude (about $1.2 \times 10^{-3}$ emu mol$^{-1}$) is reasonable as compared with the experiment (about $1.5 \times 10^{-3}$ emu mol$^{-1}$). Thus, the calculated $\chi_p$ vs. $T$ plots reproduce characteristic features revealed by the experiments by Haddon et al.[3] This in turn indicates that the calculated $J$ values, and dimer and ladder models are reliable enough for qualitative explanation of the magnetic behaviors of **1**.

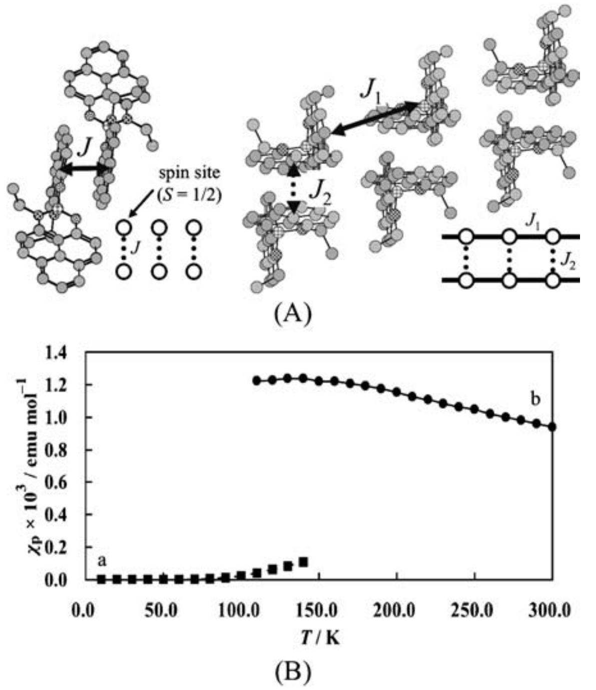

**Figure 3.** (A) Lattice models employed in the QMC simulations for **1**: dimer (left) and lattice (right) models. Both models include $S = 1/2$ spins. (B) $\chi_p$ simulated by QMC within the loop algorithm, where the squares plot data (a) obtained from the dimer lattice (256 sites), and the circle plot data (b) obtained from the ladder model ($128 \times 2$ sites).

If we use the Extended Hückel MO method, we can obtain only the orbital overlap ($s$). The transfer integral ($t$) is estimated by an empirical manner $t = \kappa s$ ($\kappa$ is usually assumed to be 10 eV). The calculated $t$ values for dimers at 100 and 173 K are 0.14 and 0.074 eV, respectively (see Table 1). The $t$ values are reasonable as compared with those of band calculations. The $U_{\mathrm{eff}}$ values can be estimated by using calculated $J$ values in eq 2: $U_{\mathrm{eff}} = 0.64$ eV at both 100 and 173 K.

Concerning the HOMO–LUMO band gaps ($E_g$), we can estimate them by assuming a linear chain, for which $E_g$ is given by $U_{\mathrm{eff}} - 4t$.[7] They are calculated by

$$E_g\ (100\,\mathrm{K}) = 0.64 - 4 \times 0.14 = 0.08\ (\mathrm{eV}), \tag{3a}$$

$$E_g\ (173\,\mathrm{K}) = 0.64 - 4 \times 0.074 = 0.344\ (\mathrm{eV}), \tag{3b}$$

Therefore, the crystal of **1** should be metallic at 100 K, while it is an insulator at 173 K. Thus, the conductivity should change dramatically, in agreement with the observed metal–insulator (Mott) transition.[3]

In conclusion, the intermolecular $J$ values of the $\pi$-dimer model has been antiferromagnetic at both lower and higher temperatures ($J = -638.5$ and $-192.1$ K, respectively). The $t$ values has been reduced by a half when temperature increases, which is consistent with the change in the conductivity. Besides, the intermolecular $J$ values of not-$\pi$ dimer models have been zero at lower temperature, while ferromagnetic at high temperature ($J = 8.3$ and 187.2 K). The QMC simulation for $\chi_p$ with using the calculated parameters has shown that these parameters are reasonable to explain magnetic behaviour of **1**, and the result has reproduced the experiment showing diamagnetism at lower temparature and paramagnetism at higher temperature. Hence, the change in the magnetism of **1** can be ascribed to the ferromagnetic interaction for the not-$\pi$ dimer at 173 K, although it is absent at 100 K. The calculated band gaps ($E_g$) are also consistent with the experiment on the conductivity.[3]

This work has been supported by a Grant-in-Aid for Scientific Research (B) (No. 19350070) form MEXT, Japan.

## References and Notes

1 R. C. Haddon, *Nature* **1975**, *256*, 394.
2 S. K. Mandal, S. Samanta, M. E. Itkis, D. W. Jensen, R. W. Reed, R. T. Oakley, F. S. Tham, B. Donnadieu, R. C. Haddon, *J. Am. Chem. Soc.* **2006**, *128*, 1982.
3 X. Chi, M. E. Itkis, K. Kirschbaum, A. A. Pinkerton, R. T. Oakley, A. W. Cordes, R. C. Haddon, *J. Am. Chem. Soc.* **2001**, *123*, 4041.
4 T. Taniguchi, T. Kawakami, K. Yamaguchi, *Polyhedron* **2005**, *24*, 2274.
5 J. Frisch, G. W. Trucks, H. B. Schlegel, G. E. Scuseria, M. A. Robb, J. R. Cheeseman, J. B. Foresman, J. Cioslowski, J. V. Ortiz, B. B. Stefanov, G. Liu, A. Liashenko, C. Gonzalez, M. Challacombe, P. M. W. Gill, B. G. Johnson, W. C. M. Head-Gordon, E. S. Replogle, J. A. Pople, *Gaussian 98*, Gaussian, Inc., Pittsburgh, PA, **2001**.
6 S. Yamanaka, T. Kawakami, H. Nagao, K. Yamaguchi, *Chem. Phys. Lett.* **1994**, *231*, 25.
7 S. Nakano, Y. Kitagawa, T. Kawakami, K. Yamaguchi, *Polyhedron* **2003**, *22*, 2027.
8 Supporting Information is available electronically on the ALPS Web site, http://alps.comp-phys.org.
9 K. Yamaguchi, M. Okumura, K. Takada, S. Yamanaka, *Int. J. Quant. Chem. Symp.* **1993**, *27*, 501.
10 K. Yamaguchi, M. Okumura, W. Mori, J. Maki, K. Takeda, T. Noro, K. Tanaka, *Chem. Phys. Lett.* **1993**, *210*, 201.

Published on the web (Advance View) June 30, 2007; doi:10.1246/cl.2007.1000